Scaling properties of multifractals as an eigenvalue problem

Mitchell J. Feigenbaum

Rockefeller University, 1230 York Avenue, New York, New York 10021

Itamar Procaccia and Tamás Tél*

Department of Chemical Physics, The Weizmann Institute of Science, Rehovot 76 100, Israel

(Received 17 November 1988)

The calculation of the scaling properties of multifractal sets is presented as an eigenvalue problem. The eigenvalue equation unifies the treatment of sets that can be organized on regular trees—be they complete or incomplete (pruned) trees. In particular, this approach unifies the multifractal analyses of sets at the borderline of chaos with those of chaotic sets. Phase transitions in the thermodynamic formalism of multifractals are identified as a crossing of the largest discrete eigenvalue with the continuous part of the spectrum of the relevant operator. An analysis of the eigenfunctions is presented and several examples are solved in detail. Of particular interest is the analysis of intermittent maps, which shows the existence of an infinite-order phase transitions, and of (Smale) incomplete maps of the interval with finite and infinite rules of pruning of the multifractal trees.

I. INTRODUCTION

Ever since it has been recognized[1-4] that fractal objects appearing in complex and nonlinear systems are not well characterized by a single scaling exponent, but rather by a spectrum of scaling exponents, there has been an explosive interest in such objects, which were termed multifractals.[3] Multifractals play a dominant role as strange attractors of chaotic dynamical systems,[5] dissipation fields of turbulent flows,[6] in growth patterns,[7,8] nonlinear resistor networks,[9] etc. The aim of this paper is to work out in detail a powerful technical tool for the study of multifractals, a tool that allows calculations of relevant scaling properties from solutions of appropriate eigenvalue equations. For dynamical systems, this tool unifies the treatment of sets at the borderline of chaos with that of systems in their chaotic regime.

The objects under study are usually fractals that support some measure. Thus for example in chaotic dynamical systems one has a limit set—a strange attractor—which is a fractal set. The natural invariant measure provides the probability that a typical orbit visits various regions of the attractor.[10] Having such "fractal measures" one can consider a coverage of the set by a partition into N balls of radii $\{l_i\}_{i=1}^{N}$, each of which having a measure p_i. If one introduces a partition function[2,4]

$$\Gamma(\{l_i\}, q, \tau) = \sum_{i=1}^{N} p_i^q / l_i^{\tau} , \qquad (1.1)$$

it can be shown that in the appropriate $N \to \infty$ limit this partition function is either zero or infinity depending on whether $\tau > \tau(q)$ or $\tau < \tau(q)$. This defines $\tau(q)$. It has been shown further that the function $\tau(q)$ furnishes important information about the scaling properties of fractal measures. In particular a Legendre transform of $\tau(q)$ yields the $f(\alpha)$ function, a very convenient representa-

tion of the scaling properties of fractal measures.[4]

Simple and elegant theories to calculate $\tau(q)$ [or, in fact, its inverse function $q(\tau)$], have been developed when the partition is an equimeasure partition, i.e., where $p_i = \mathrm{const} = 1/N$.[11-13] Such a situation occurs, for example, at the accumulation point of period doubling, where $N = 2^n$ at the nth generation of refinement of the partition. Since in practice one calculates $q(\tau)$ by requiring that $\Gamma(q, \tau) = 1$, one can rewrite Eq. (1.1) in such a case as

$$2^{nq(\tau)} \sim \sum_{i=1}^{N} l_i^{-\tau} . \qquad (1.2)$$

In general, the number of balls in a partition is not increasing with the generations necessarily like 2^n, but rather like a^n, where a can be any real number. Then Eq. (1.2) turns to

$$a^{nq(\tau)} \sim \sum_{i=1}^{N} l_i^{-\tau} . \qquad (1.3)$$

Inspecting Eq. (1.2) or (1.3) one notices the resemblances to the statistical mechanical relation

$$e^{-nG(\beta)} = \sum_{i} e^{-\beta E_i} , \qquad (1.4)$$

where $G(\beta)$ is the free energy (density) multiplied by the inverse temperature β. Indeed, this resemblance gave rise to the development of the thermodynamic formalism of multifractals.[14,15] In particular $a^{q(\tau)}$ can be calculated as the largest eigenvalue of a transfer matrix of an appropriate spin model whose thermodynamics is equivalent to that of the given fractal measure. Nonanalyticities in $q(\tau)$ could be interpreted as phase-transitions.[16-19]

If the partitions are not equimeasure partitions, $q(\tau)$ cannot be calculated in this way. Still, the rate of growth of the sum $\sum_i l_i^{-\tau}$ is an important piece of information on the multifractal set, shedding light on its geometric re-

scaling factors. To avoid confusion with $q(\tau)$ we shall adopt a different notation for this rate of growth, a notation that follows standard thermodynamics. We shall write,

$$e^{-nG(\beta)} = \sum_{i=1}^{a^n} l_i^{\beta} . \tag{1.5}$$

$G(\beta)$ might depend on the partition. For point sets organized on regular trees, we shall use the coverage defined in Sec. II. We stress that for problems for which $p_i = $const there is a correspondence $\tau \leftrightarrow -\beta$, $G(\beta) \leftrightarrow -q(-\beta)\ln a$. Otherwise, we are dealing with different functions, cf. Sec. III D. In fact, for the generating partition of hyperbolic systems, $-G(\beta)$ is a quantity called pressure in the mathematical literature of thermodynamic formalism and has extensively been studied.[14,15] The sum (1.5) has already been investigated for nonhyperbolic systems, too, and it has been found that $G(\beta)$ can have nonanalyticities (phase transitions) as well.[20]

The theory developed below is aimed at calculating the function $G(\beta)$. It will be seen that one can write eigenvalue equations using an operator whose largest eigenvalue is $e^{-G(\beta)}$. The eigenfunctions are interesting, and their analysis will shed light on the free energy $G(\beta)$ and on other eigenvalues in this formalism. The theory developed below is valid for sets that can be organized on regular trees—binary, ternary, or higher-order trees. There is no requirement that the trees be complete; the number of legs can grow at a rate slower than 2^n, 3^n, etc. In such cases we shall need the rules of pruning of the trees in order to write a close-form theory.

In Sec. II we derive the eigenvalue equations for complete trees. Section III discusses applications to dynamical systems which are (Smale) complete maps of the interval. In Sec. IV a detailed discussion of the singularities of the eigenfunctions is performed. It yields an understanding of the space of functions in which the eigenvalue equations operate, and the nature of the discrete and continuous components of the spectra. Section V is devoted to the study of intermittent maps and the interesting phase transition in their thermodynamic functions. It is shown that this phase transition is identical to the one found in the context of mode lockings of quasiperiodic systems, and that it has an equivalent number theoretic representation. The eigenvalue equations allow us a solution of the phase transition, which turns out to be of infinite order. Section VI treats incomplete maps of the interval where the pruning of the trees is vital. It is easy to accomplish a calculation of the thermodynamic functions when the itinerary of the critical point is periodic or preperiodic. However, when the itinerary is aperiodic one has to resort to indirect methods. The method suggested in Sec. VI relies on calculations at parameter values for which the itineraries are periodic, but with increasing length of the period. It is shown that such calculations converge. Section VII is a summary and discussion.

II. EIGENVALUE EQUATIONS

We consider here point-sets that can be organized on regular trees, such that at the nth level there are exactly

k^n points in the set, with k integer, $k \geq 2$. Then every point in the nth generation can be given an address $(\epsilon_n, \epsilon_{n-1}, \ldots, \epsilon_1)$, where ϵ_i is an index that takes on k values $(0, 1, \ldots, k-1)$. (See Fig. 1 for a binary tree example.) This address can be also converted into a number t,[11,12]

$$t = \sum_{j=1}^{n} \epsilon_j k^{n-j} . \tag{2.1}$$

Assume also that there are k given functions F_ϵ, that can be used to find the points of the $(n+1)$th generation from the points of the nth generation

$$x_t^{(n)} = \begin{cases} F_0 \\ \quad \to \quad x_{kt}^{(n+1)} \\ F_1 \\ \quad \to \quad x_{kt+1}^{(n+1)} \\ \vdots \\ F_{k-1} \\ \quad \to \quad x_{kt+(k-1)}^{(n+1)} . \end{cases} \tag{2.2}$$

Finally, assume that there exists a unique "seed" point x^* of the zeroth generation, from which all points of the nth generation can be constructed. This choice of generation through the functions F_ϵ, called elsewhere[21] "pre-
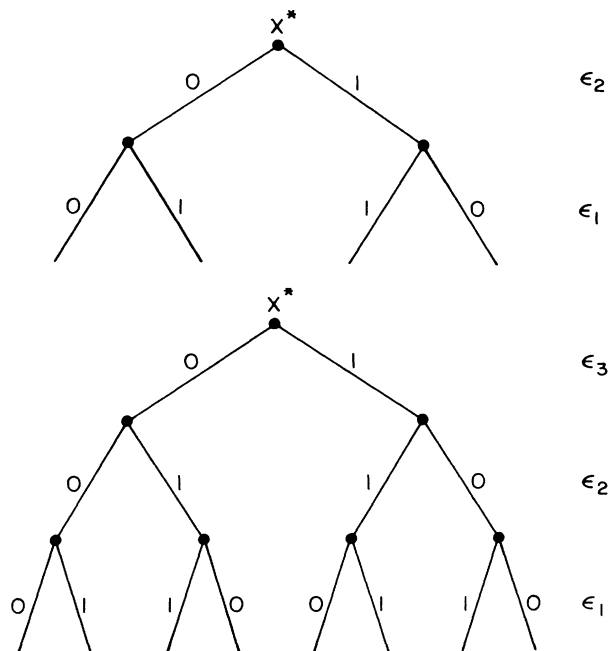

FIG. 1. An example of a binary tree and the labeling used in this paper. A transition from generation to generation is associated with shifting the ϵ_i's as shown. Each point of the set is obtained from the seed x^* as a result of a composition of the presentation functions F_ϵ, in the order shown, i.e., $x^{(n)}(\epsilon_n, \ldots, \epsilon_1) = F_{\epsilon_1} \circ \cdots \circ F_{\epsilon_n}(x^*)$. Note, however, that the x values obtained in this way need not be ordered along the x axis.

sentation functions," has dynamical foundations which are expounded in Ref. 21. These connections ensure that the machinery developed in this paper is directly pertinent to a large variety of significant dynamical problems. Given the functions F_ϵ, we can write

$$x_t^{(n)} \equiv x^{(n)}(\epsilon_n, \epsilon_{n-1}, \ldots, \epsilon_1) = F_{\epsilon_1} \circ F_{\epsilon_2} \circ \cdots \circ F_{\epsilon_n}(x^*) ,$$

(2.3)

Where the symbol $\circ$ denotes a composition, $F \circ F(x) = F(F(x))$. We shall assume that a partition at the nth generation is obtained from balls of diameter $l^{(n)}(\eta, \epsilon_{n-1}, \ldots, \epsilon_1)$,

$$l^{(n)}(\eta, \epsilon_{n-1}, \ldots, \epsilon_1)$$
$$= |F_{\epsilon_1} \circ F_{\epsilon_2} \circ \cdots \circ F_{\epsilon_{n-1}}(F_\eta(x^*))$$
$$- F_{\epsilon_1} \circ F_{\epsilon_2} \circ \cdots \circ F_{\epsilon_{n-1}}(F_\xi(x^*))| ,$$

(2.4)

where $\eta = 1, \ldots k - 1$ and $\xi = \eta - 1$.

This calculation of a ball diameter relies on the fact that F_ϵ is contractive. Thus distances between nearest points are naturally obtained by Eq. (2.4) as a consequence of the exponential growth of stability of a composition of F_ϵ's. For n sufficiently large Eq. (2.4) behaves asymptotically according to the chain rule as

$$l^{(n)}(\eta, \epsilon_{n-1}, \ldots, \epsilon_1)$$
$$\sim |F'_{\epsilon_1}(F_{\epsilon_2} \circ F_{\epsilon_3} \cdots) F'_{\epsilon_2}(F_{\epsilon_3} \circ F_{\epsilon_4} \cdots) \cdots | .$$

(2.5)

We are now in position to derive the eigenvalue equation. Consider the sum

$$S(n, \beta) = \sum_{\eta, \ldots, \epsilon_{n-1}} \lambda^{-n}(\beta) [l^{(n)}(\eta, \epsilon_{n-1}, \ldots, \epsilon_1)]^\beta .$$

(2.6)

Using Eq. (2.5) we can estimate $S(n, \beta)$ as

$$S(n, \beta) \sim \cdots \sum_{\epsilon_r} \lambda^{-1}(\beta) |F'_{\epsilon_r}(F_{\epsilon_{r+1}} \cdots)|^\beta \sum_{\epsilon_{r-1}} \lambda^{-1}(\beta) |F'_{\epsilon_{r-1}}(F_{\epsilon_{r-1}} F_{\epsilon_{r+1}} \cdots)|^\beta \cdots .$$

(2.7)

To proceed, adopt the following notation:

$$\psi_r^{(\beta)}(F_{\epsilon_r} \circ F_{\epsilon_{r+1}} \circ \cdots)$$
$$\equiv \sum_{\epsilon_{r-1}} \lambda^{-1}(\beta) |F'_{\epsilon_{r-1}}(F_{\epsilon_r} \circ F_{\epsilon_{r+1}} \circ \cdots)|^\beta$$

(2.8)

and

$$x = F_{\epsilon_{r+1}} \circ \cdots \circ F_{\epsilon_{n-1}} \circ F_{\epsilon_n}(x^*) .$$

(2.9)

With this notation the terms shown on the right-hand side of (2.7) yield precisely $\psi_{r+1}^{(\beta)}(x)$. Also, written explicitly, these terms read

$$\psi_{r+1}^{(\beta)}(x) = \sum_\epsilon \lambda^{-1}(\beta) |F'_\epsilon(x)|^\beta \psi_r^{(\beta)}(F_\epsilon(x)) .$$

(2.10)

Finally, assuming convergence in the limit $r \to \infty$, we can write the functional eigenvalue equation

$$\lambda(\beta) \psi^{(\beta)}(x) = \sum_\epsilon |F'_\epsilon(x)|^\beta \psi^{(\beta)}(F_\epsilon(x)) .$$

(2.11)

The number $\lambda(\beta)$ is an eigenvalue. Defining the linear operator $L^{(\beta)}$ via

$$L^{(\beta)} \psi(x) = \sum_\epsilon |F'_\epsilon(x)|^\beta \psi(F_\epsilon(x)) ,$$

(2.12)

we realize that $\lambda(\beta)$ is the largest eigenvalue of $L^{(\beta)}$. On the other hand, the statement that for large r, $\psi_{r+1} \sim \psi_r$ is equivalent to requiring that $\sum_i \lambda^{-n} |l_i^{(n)}|^\beta \sim 1$, or [cf. Eq. (1.5)]

$$\lambda(\beta) = e^{-G(\beta)} ,$$

(2.13)

where $G(\beta)$ is the thermodynamic function associated with the coverage (2.4). We shall be interested both in the eigenvalues $\lambda(\beta)$ and in the eigenfunctions $\psi^{(\beta)}(x)$. We have to study now the space of functions that we ex-

pect $\psi^{(\beta)}(x)$ to occupy, and what kind of spectrum $\lambda(\beta)$ belongs to it. To this aim we turn now to some concrete examples.

III. APPLICATIONS TO DYNAMICAL SYSTEMS: COMPLETE MAPS OF THE INTERVAL

A. Preliminary details

Consider the family of one-hump maps $f(x)$ which map the interval onto itself (Smale complete maps) and generate chaotic dynamics. A particular branch of this family is given by the maps

$$x' = 1 - |1 - 2x|^z ,$$

(3.1)

on the interval $[0,1]$ for $z \geq \frac{1}{2}$. A set that conforms with the assumptions of Sec. II is the set of all the preimages of the critical point $x_c = \frac{1}{2}$, $x^* = x_c$. The two functions F_0 and F_1 which transfer x_t into x_{2t} and x_{2t+1} are the two inverses of the function $f(x)$. For the family (3.1) the functions $F_\epsilon(x)$ are

$$F_\epsilon(x) = \frac{1}{2} + (\epsilon - \frac{1}{2})(1 - x)^{1/z} ,$$

(3.2)

where ϵ takes on the two values 0 and 1.

To write the eigenvalue equation in this case, we have to find $F'_\epsilon(x)$. For the problem at hand these derivatives can be written as

$$F_\epsilon =' \frac{1}{f'(F_\epsilon(x))} .$$

(3.3)

Accordingly, Eq. (2.10) takes on the form

$$\lambda(\beta) \psi_{n+1}^{(\beta)}(y) = \sum_{x \in f^{-1}(y)} \frac{\psi_n^{(\beta)}(x)}{|f'(x)|^\beta} .$$

(3.4)

Once written, this equation is immediately recognized as a generalization of the Frobenius-Perron equation[22] which is obtained in the limit $\beta = 1$, $\lambda(1) = 1$. Different extensions of the Frobenius-Perron equation have been used in the context of transient chaotic behavior.[23] For nonhyperbolic maps Eq. (3.4) has been introduced in Ref. 24 where it was shown that for smooth initial functions ψ_0 there exists one and only one coefficient $\lambda(\beta)$ so that the series of $\psi_n^{(\beta)}$ converges (exponentially fast) toward a finite $\psi^{(\beta)}(x)$, i.e., both $\lambda(\beta)$ and $\psi^{(\beta)}$ are unique, and furthermore, that for hyperbolic maps $\lambda(\beta)$ yields the spectrum of generalized entropies[25] for both permanent and transient chaos. [We call a map hyperbolic if $1 < |f'(x)| < \infty$ holds.]

The operator $L^{(\beta)}$ of Eq. (2.12) which is now a special case of Ruelle's Frobenius-Perron operator,[14] takes on the form

$$L^{(\beta)}Q(y) = \sum_{x \in f^{-1}(y)} \frac{Q(x)}{|f'(x)|^\beta} . \tag{3.5}$$

The largest eigenvalue of it $\lambda(\beta)$, is connected via Eq. (2.13) with $G(\beta)$ of the length scale partition sum (1.5) on the coverage defined by (2.4). It is to be noted that (2.4) provides a partial coverage of the attractor which, therefore, differs slightly from the coverage of the generating partition used for one-hump maps.[14,15] The thermodynamics for these partitions are, however, expected to be the same.

Below we shall find it advantageous to consider the whole spectrum of $L^{(\beta)}$ and eigenfunctions belonging to eigenvalues other than the largest. Before we do that, however, we examine some numerical solutions of Eq. (3.4).

B. Numerical solutions

Equation (3.4) can be solved numerically in a straightforward way. Since the limit is unique, we can start with an initial function $\psi_0 \equiv 1$. At all levels ψ_n is normalized such that $\psi_n(\tilde{x}) = 1$ for some suitable $\tilde{x}$. We approach $\psi^{(\beta)}(x)$ through a sequence of functions $\psi_n(x)$ which transform according to

$$\psi_{n+1}(x) = \sum_\epsilon |F'_\epsilon(x)|^\beta \psi_n(F_\epsilon(x))/\lambda_n , \tag{3.6}$$

where

$$\lambda_n = \sum_\epsilon |F'_\epsilon(\tilde{x})|^\beta \psi_n(F_\epsilon(\tilde{x})) . \tag{3.7}$$

The series of λ_n tends simultaneously to the largest eigenvalue $\lambda(\beta)$. This transformation is numerically accomplished through a recursive function call. In the next section we discuss the eigenfunctions $\psi^{(\beta)}(x)$ themselves. Here we display the results for $\lambda(\beta)$ of the procedure described above.

Example (i). As a first example we take $z = 2$ in Eq. (3.1). This parabolic case yields well-known thermodynamics and we present it here as a check.

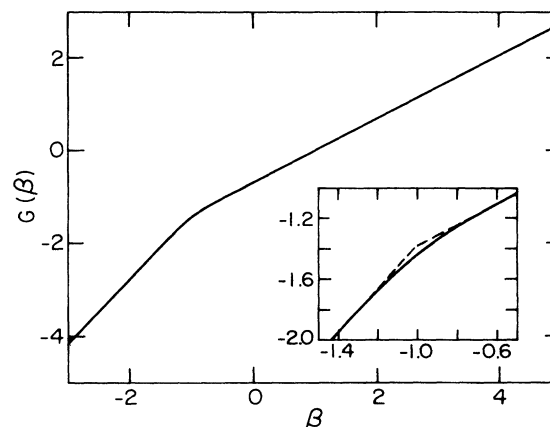Figure 2 displays $G(\beta)$ versus β. The analytic solution in this case reads[15,17,24]

FIG. 2. $G(\beta)$ vs β for the quadratic, complete map, as obtained from $\lambda_{16}(\beta)$ of Eq. (3.7). In the inset the vicinity of the phase transition is enlarged and the dashed line is the exact solution for $-q(-\beta)\log 2$.

$$G(\beta) = \begin{cases} 2\beta \ln 2 & \beta < -1 \\ (\beta - 1)\ln 2 & \beta > -1 \end{cases} \tag{3.8}$$

and the numerics agree very well. Convergence is fast except near the phase transition point $\beta_c = -1$ where the difference between the numerics and (3.8) is still seen (and is of the order of 4%) even after 16 iterations.

Example (ii). Here we take $z = 4$. There is no analytic solution for the whole β axis, and the numerical solution is displayed in Fig. 3. Notice that the left branch appears to be straight as in Fig. 2, whereas the right branch is curved. The theory of Sec. IV will verify these numerical findings.

C. Fair warning about measures

The natural invariant measures of maps of the family (3.1) all have singularities at $x = 0, 1$ such that for $x \sim \epsilon$ or
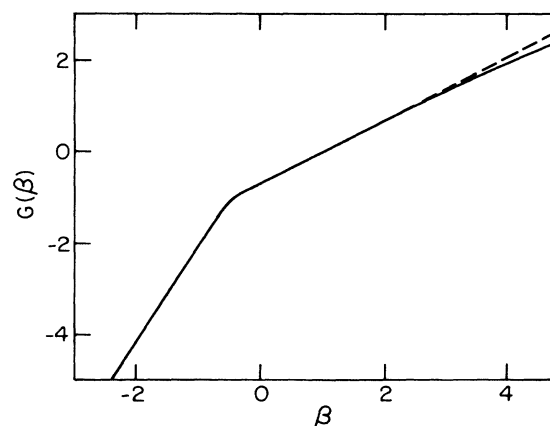

FIG. 3. $G(\beta)$ vs β for the quartic complete map with $z = 4$, obtained from $\lambda_{16}(\beta)$. The dashed line, which is simply $(\beta - 1)\log 2$, is put to stress the fact that the right branch is curving.

$x \sim 1-\epsilon$, $\psi^{(1)}(x) \sim \epsilon^{-(1-1/z)}$ (cf. Sec. IV). Thus any partition owns two boxes of size l at the extremes of the interval whose measure $P(l)$ scales as $P(l) \sim l^{\alpha}$ with $\alpha = 1/z$. All other boxes have nonsingular measures with $\alpha = 1$. In the notation of Ref. 4, $\tau(q)$ of Eq. (1.1) reads (for $z > 1$)

$$\tau(q) = q\alpha - f(\alpha) = \begin{cases} q/z, & q > z/(z-1) \ , \\ q-1, & q < z/(z-1) \ . \end{cases} \quad (3.9)$$

As noted before for cases where the partition is an equimeasure partition, $G(\beta) = -q(-\beta)\ln 2$. This is indeed the case for example (i), but is not so for example (ii). The reason for the different thermodynamics is that the partition via the preimages of the critical point contains boxes with singularly nonconstant natural measures at both ends. We reiterate this fact to stress the difference in general between $G(\beta)$ and $q(\tau)$.

IV. SINGULARITY ANALYSIS OF THE EIGENFUNCTIONS

The understanding of the thermodynamics and the eigenvalue equations calls for some careful examination of the nature of the eigenfunctions, the spaces of functions from which they are drawn, and the spectrum of eigenvalues which characterizes the operator (3.5). The insight provided by analyses of the Frobenius-Perron equation (the $\beta \to 1$ limit) cannot be taken over in cases where use is being made of the fact the $\psi^{(1)}(x)$ is a normalized density. Rather, we shall see that in general the singularities of $\psi^{(\beta)}(x)$ shed important light on the nature of classification needed for these eigenfunctions. In addition, we shall see that eigenvalues different from the largest one own eigenfunctions whose nature reveals aspects of the thermodynamics in a very useful way.

A. Space of legal eigenfunctions

In this subsection we show that functions that have different singularities at $x = 0, 1$ belong to a special class, which gives rise to a continuous component of the spectrum. Functions with identical singularities belong to the discrete spectrum. The distinction will be shown to be natural since initial functions which are smooth are orthogonal to the functions of the special class.

To see this, consider the general family of one-hump maps on the interval. We shall assume that the maximum of the map at $x = x_c$ is of the order z, i.e., near the maximum $f(x) = 1 - a|x - x_c|^z$, $a > 0$. In addition, the slopes of the function at $x = 0, 1$ will be denoted by c, c_1, respectively, see Fig. 4. It will be seen that the qualitative analysis depends solely on the order of the maximum and the values of these slopes. Our analysis is an extension of what was applied to the Frobenius-Perron equation.[26] In particular, to analyze $\psi^{(\beta)}(y)$ via Eq. (3.4) we shall need the inverse functions at $y \to 0, 1$.

(i) The inverse for $y \to 1$: For $y \to 1$ the two preimages are

$$x_{1,2} = x_c \pm \left[\frac{1-y}{a} \right]^{1/z} . \quad (4.1)$$
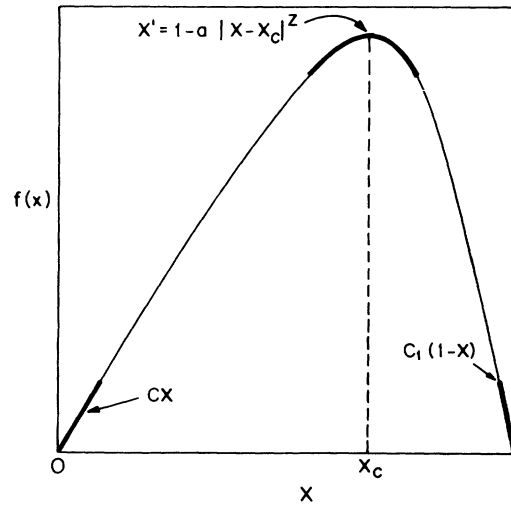

FIG. 4. A sketch of a typical one-hump map of the interval $(0,1)$. The theory depends crucially on the order of the maximum z and on the slopes c and c_1.

The derivatives $f'(x)$ at these points are

$$|f'(x_{1,2})| = a^{1/z} z |1-y|^{1-1/z} . \quad (4.2)$$

(ii) The inverse for $y \to 0$: For $y \to 0$ the two preimages are

$$x_1 = \frac{y}{c} ,$$

$$x_2 = 1 - \frac{y}{c_1} . \quad (4.3)$$

The derivatives at these points are

$$f'(x_1) = c ,$$

$$f'(x_2) = -c_1 . \quad (4.4)$$

With these preliminaries we can ask what is the fate of an initial function $\psi_0(x)$, under $L^{(\beta)}$ with a given λ. In particular, we want to know how $\psi_n^{(\beta)}(y)$ behaves for $y \to 0, 1$.

Using Eq. (4.1) and (4.2), we can conclude that if $\psi_n^{(\beta)}(x)$ is smooth around x_c then

$$\psi_{n+1}^{(\beta)}(y) \underset{y \to 1}{\sim} \frac{2\lambda^{-1}\psi_n(x_c)}{(za^{1/z})^{\beta}}(1-y)^{-(1-1/z)\beta} . \quad (4.5)$$

On the other hand, in the limit $y \to 0$, we find

$$\psi_{n+1}^{(\beta)}(y) \underset{y \to 0}{\sim} \lambda^{-1} \left[\frac{\psi_n^{(\beta)}(y/c)}{c^{\beta}} + \frac{\psi_n^{(\beta)}(1-y/c_1)}{c_1^{\beta}} \right] . \quad (4.6)$$

Allow now $\psi_0(x)$ to have singularities of strength α_0 and σ_0 at the two ends,

$$\psi_0(x) \underset{x \to 0}{\sim} A_0(x)^{-\alpha_0}, \quad \psi_0(x) \underset{x \to 1}{\sim} B_0(1-x)^{-\sigma_0} \quad (4.7)$$

and watch what happens upon iterations.
$n = 1$:

$$\psi_1^{(\beta)}(y) \underset{y \to 1}{\sim} (1-y)^{-\sigma} , \quad (4.8)$$

where $\sigma = (1 - 1/z)\beta$ is what we call the "natural" singularity,

$$\psi_1^{(\beta)}(y) \underset{y \to 0}{\sim} \lambda^{-1} \left[\frac{A_0}{c^\beta}(y/c)^{-\alpha_0} + \frac{B_0}{c_1^\beta}(y/c_1)^{-\sigma_0} \right] . \quad (4.9)$$

In the last expression one of the singularities dominates as $y \to 0$, and we write

$$\psi_1^{(\beta)}(y) \underset{y \to 0}{\sim} (y)^{-\alpha_1}, \quad \alpha_1 = \max(\alpha_0, \sigma_0) . \quad (4.10)$$

$n = 2$: Upon the second iteration the singularity of $\psi_2^{(\beta)}(y)$ for $y \to 1$ is not changing; at the other corner we find

$$\psi_2^{(\beta)}(y) \underset{y \to 0}{\sim} (y)^{-\alpha}, \quad \alpha = \max(\alpha_1, \sigma) . \quad (4.11)$$

These types of singularities are not altered upon further iterations.

We can thus conclude that there are two types of initial functions $\psi_0(x)$, which we designate as follows.

Class A: $\alpha_1 < \sigma$; this class of functions iterates to functions having the same singularities at both ends.

Class B: $\alpha_1 > \sigma$; this class of functions iterates to functions having two different types of singularities, $\alpha \neq \sigma$ at two ends.

Notice that since σ is β dependent these classes are also β dependent. In Sec. IV B we focus on class A. Here we show that class B belongs to the continuous spectrum of the operator (3.5).

To see this we consider $\psi^{(\beta)}(y)$ obtained after many iterations $(n \to \infty)$ in the limit $y \to 0$,

$$\psi^{(\beta)}(y) - \frac{\lambda^{-1}}{c^\beta}\psi^{(\beta)}(y/c) = \frac{\lambda^{-1}}{c_1^\beta}\psi^{(\beta)}(1 - y/c_1) . \quad (4.12)$$

From Eq. (4.5) we know that the right-hand side has singularity of strength σ. The equation can be balanced with a left singularity of strength α only if

$$1 - \frac{\lambda^{-1}}{c^{\beta-\alpha}} = 0 \quad (4.13)$$

or

$$\lambda^{-1} = c^{\beta-\alpha} . \quad (4.14)$$

Since λ^{-1} can be chosen arbitrarily, this eigenvalue, if it exists, belongs to the *continuous* spectrum (The latter is a new type of continuum different from what is called the continuous spectrum of the Frobenius-Perron operator in the mathematical literature.[14]) On the other hand, if $\alpha = \sigma$, λ^{-1} cannot be expressed in terms of c. These functions, which belong to class A, belong to the *discrete* spectrum.

The last issue of analysis is the question when can one reach functions of class B upon iterations starting with $\psi_0(x)$ belonging to the class. Denoting the eigenvalues in the discrete spectrum by $\lambda_i(\beta)$, with $\lambda_1(\beta)$ being the largest, we note that only if λ of Eq. (4.14) is larger, i.e.,

$$c^{\alpha-\beta} > \lambda_1(\beta) , \quad (4.15)$$

then the function $\psi_0(x)$ remains within the class. Other-

wise, it turns automatically to a function of class A. Then, also, starting with a function of class A the iteration stays within the class. We turn now to an analysis of the discrete spectrum, stressing that as a function of β one can observe transitions between solutions belonging to the two classes. These transitions are strongly related to phase transitions in the thermodynamic formalism.

B. Discrete spectrum and its eigenfunctions

The discrete spectrum belongs to eigenfunctions of class A. Initial conditions $\psi_0(x)$, which are of this class and are non-negative everywhere, remain in the class under iterations.

The analysis of the discrete spectrum and the eigenfunctions is facilitated by studying conjugations to different maps and in particular to hyperbolic maps[27] (i.e., maps which must have a maximum of order $z = 1$). The details of the conjugation and its effects on the eigenfunctions are presented in Appendix A. Here the main results are summarized.

The complete maps $f(x)$ and $g(x)$ of the interval are called conjugate if there exists a function $h(x)$ such that

$$f(x) = h^{-1} \circ g \circ h(x) . \quad (4.16)$$

If $\psi_f^{(\beta)}(x)$ and $\psi_g^{(\beta)}(x)$ are eigenfunctions belonging to (3.4) with f and g, respectively, then

$$\psi_f^{(\beta)}(x) = \psi_g^{(\beta)} \circ h(x) |h'(x)|^\beta , \quad (4.17)$$

and the associated eigenvalues are invariant to conjugation. It is of particular importance that one can choose a function h such that the conjugation leads from nonhyperbolic to a hyperbolic map as pointed out in Ref. 28. Having a nonhyperbolic map $f(x)$ whose invariant density is $\psi^{(1)}(x)$, one defines

$$\tilde{h}(x) = \int_0^x \psi^{(1)}(y)dy \quad (4.18)$$

and then conjugating as in Eq. (4.16) leads to a hyperbolic map $g(x) = \tilde{f}(x)$. The discrete spectrum of hyperbolic maps is always associated with smooth (i.e., nonsingular) eigenfunctions $\psi_g^{(\beta)}$. The conjugation maps the spectrum of the hyperbolic map onto the spectrum of the nonhyperbolic map, while via Eq. (4.17) the eigenfunctions will gain the singularities typical of class A. Since $\psi^{(1)}(x)$ has singularities of strength $(1 - 1/z)$, the eigenfunctions will have singularities of strength $(1 - 1/z)\beta$ as calculated in Sec. II A.

The considerations above make it possible to establish a relation between $\lambda_1(\beta)$ and the generalized entropies K_β.[25] The latters can be expressed in terms of the conjugate map $\tilde{f}$.[27,29] In the special case of hyperbolic maps, the eigenvalue of (3.4) obtained by starting with any smooth initial function has been shown to be directly related to K_β.[24,27,30] More generally, for any chaotic map one obtains

$$\ln\lambda_1(\beta) = (1 - \beta)K_\beta , \quad (4.19)$$

where $\lambda_1(\beta)$ is the eigenvalue of the operator $\dot{H} = (\psi^{(1)})^{-\beta}L^{(\beta)}(\psi^{(1)})^\beta$ reached from a constant initial function,[27] i.e., in the formulation of the present paper,

$\lambda_1(\beta)$ is the largest eigenvalue of the discrete spectrum (associated with functions of class A).

C. Observed thermodynamics

We are now in position to examine the thermodynamics which is obtained upon iterating the functional equation with a smooth initial function. Of importance is the competition between the discrete and continuous part of the spectrum.

By starting with a smooth function $\psi_0(x)$, its first iterate will possess a singularity of strength σ at $x = 1$ as explained in Sec. IV A, but will be constant at the left corner. The singularity at $x = 1$ will not be removed by further iterations. Let us follow what happens to $\psi_n^{(\beta)}(0)$. By applying Eq. (4.6) for $n = 1$ we see that the behavior of $\psi_2^{(\beta)}$ at $x \to 0$ depends on the actual sign of σ. For $\sigma > 0$, the second term dominates on the right-hand side and this leads to a singularity of strength σ, also, at $x = 0$, which stays there forever. Thus, smooth initial functions are mapped after two steps on class A and, therefore, their evolution is governed by the discrete spectrum. In particular, the asymptotic behavior is characterized by $\lambda_1(\beta)$ in the case where $\sigma > 0$ ($\beta > 0$ for $z > 1$).

The situation is quite different for $\sigma < 0$ since $\psi_1^{(\beta)}(x)$ then does not diverge for $x \to 1$, but rather vanishes. Therefore, $\psi_2^{(\beta)}$ will stay constant at $x = 0$. Its further fate depends on the actual value of β.

Smooth initial functions in the range $\sigma < 0$ are, thus, iterated not in class A but rather in a subclass of class B, namely in the class of functions which are constant at $x = 0$ and have singularities of strength σ at $x = 1$. It follows then from (4.6) that the eigenvalue inside this subclass is

$$\lambda = \lambda_0(\beta) = c^{-\beta} . \tag{4.20}$$

In fact, this is a special case of (4.14). Since $\lambda_0(\beta)$ is unique at all β, where it exists, we can say that the continuum spectrum restricted to the subclass appears as an "effective" *discrete* branch $\lambda_0(\beta)$. This means that, for $\sigma < 0$, $\lambda_0(\beta)$ is to be added to the discrete spectrum when starting with smooth initial functions. In the range where $\lambda_0(\beta) < \lambda_1(\beta)$, the latter dominates. In Eq. (4.6) $\lambda = \lambda_1(\beta) > c^{-\beta}$, therefore, $\psi_n^{(\beta)}(0)$ will tend to zero and the limiting function $\psi^{(\beta)}(x)$ will belong to class A. If, however, $\lambda_0(\beta) > \lambda_1(\beta)$, λ_0 dominates, and $\psi^{(\beta)}$ will belong to the subclass introduced above. The observed thermodynamics is connected with the actually largest eigenvalue, i.e.,

$$e^{-G(\beta)} = \lambda(\beta) = \max(\lambda_0(\beta), \lambda_1(\beta)) . \tag{4.21}$$

Thus, an essentially different behavior can be observed on two sides of a critical temperature β_c for which

$$\lambda_1(\beta_c) = c^{-\beta_c} . \tag{4.22}$$

Therefore, the phenomenon can be interpreted as a (first-order) phase transition and the region $\beta/\beta_c > 1$ can be called the condensed phase.

As we saw, initial functions of class A do not leave this class. In other words, the largest eigenvalue influencing their evolution is always $\lambda_1(\beta)$. This provides a useful method for calculating $\lambda_1(\beta)$, i.e., the spectrum of generalized entropies. By starting with, e.g., $\bar{\psi}_0(x) = x^{-\sigma}(1-x)^{-\sigma}$, the analogue of (3.6) and (3.7) defines a series $\bar{\psi}_n(x)$ tending to a (finite) function of class A (see also Ref. 27). $\lambda_1(\beta)$ can then be obtained as the limit of the λ_n as given by (3.7). It is worth emphasizing that in this procedure no critical slowing down appears at β_c in contrast to what one sees with a smooth initial function. The critical value can then be determined with a high accuracy as the intersection of two branches [see (4.21)]. These branches are shown on Fig. 5 for the example (ii) of Sec. III. We conclude by showing a qualitative sketch indicating the change of behavior of the eigenfunctions along different branches on Fig. 6. We note that one cannot exclude the situation where $\lambda_0(\beta)$ is always less than $\lambda_1(\beta)$. In such cases there would be no phase transition.

V. THERMODYNAMICS OF INTERMITTENT MAPS

In this section we discuss the eigenvalue equation and the thermodynamics for complete maps of the interval which are strongly nonhyperbolic, in the sense that a fixed point is marginally stable and the orbits are intermittent.[31] The set obtained displays a phase transition whose nature has been hitherto elusive. This phase transition is of more general interest because an identical kind of phase transition appears in other, seemingly unrelated, problems. In Appendix B it is shown that the thermodynamics of the set provided by the rational numbers in the Farey model, which is also the thermodynamics of the set which appears in the treatment of mode-locking of
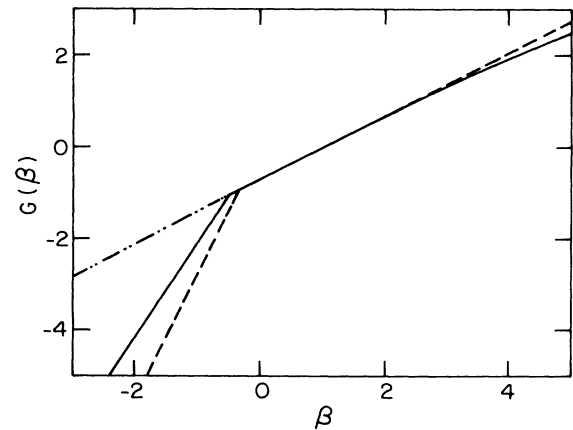

FIG. 5. The observed thermodynamics for the quartic map. The continuous branches are determined by the leading eigenvalues λ_0 for the left branch and λ_1 for the right branch. The λ_1 branch is continued in a dashed-dotted line. The whole $\lambda_1(\beta)$ branch corresponds to the generalized entropies K_β, cf. text. The dashed line is $-q(-\beta)\ln 2$, which is the thermodynamics of the invariant measure, and is added to illustrate the warning of Sec. III C. The nonanalyticity appears at a different value of β in the two cases.
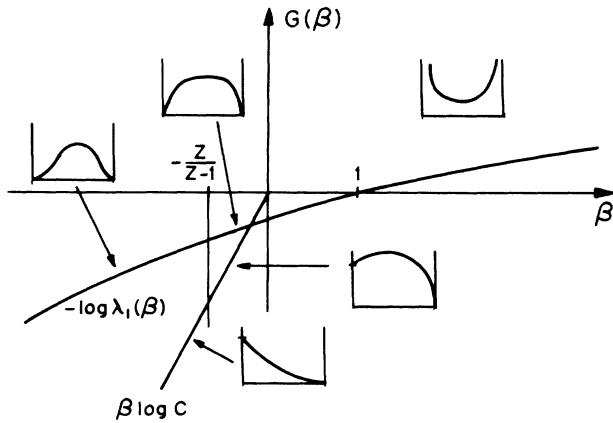
FIG. 6. A sketch of the eigenfunctions pertaining to different regions of β, $G(\beta)$, for a case with $z > 1$.

coupled nonlinear oscillators, conforms exactly with that of the intermittent map.

In principle, any map of the interval that starts as $x + x^2 + \cdots$ can be used to observe intermittency. The analysis of the number-theoretic Farey model in Appendix B suggests the use of the map

$$x' = \begin{cases} \dfrac{x}{1-x}, & x < \tfrac{1}{2} \\[2mm] \dfrac{1-x}{x}, & x > \tfrac{1}{2} \ . \end{cases} \tag{5.1}$$

Since $g(x) = x/(1-x)$ is known to be the fixed point of the intermittency renormalization group,[32] we can use it to derive statements that have universal applicability to intermittent maps. As far as intermittency is concerned the choice of the right-hand branch is irrelevant as long as it provides reinjection to $x \sim 0$. The choice in Eq. (5.1), which is motivated by the number theoretic analysis, provides, however, important symmetry properties which are used in the solution below.

Denoting $(0, \tfrac{1}{2})$ by 0 and $(\tfrac{1}{2}, 1)$ by 1, we can write the inverses of the functions in (5.1) as

$$F_0(x) = \frac{x}{1+x} \ ,$$
$$F_1(x) = \frac{1}{1+x} = 1 - F_0(x) \ . \tag{5.2}$$

All we need do now is write down the functional eigenvalue equation for (5.2) which reads

$$\lambda(\beta)\psi^{(\beta)}(x)$$
$$= (1+x)^{-2\beta}\left[\psi^{(\beta)}\left[\frac{x}{1+x}\right] + \psi^{(\beta)}\left[\frac{1}{1+x}\right]\right] \ . \tag{5.3}$$

Notice first that for $\beta = 1$, $\psi^{(1)}$ simply has a pole at the origin,

$$\beta = 1 \rightarrow \psi^{(1)}(x) = 1/x \rightarrow \lambda = 1 \ . \tag{5.4}$$

Next, for $\beta = -m/2$, $m = 0, 1, \ldots$, (5.3) possesses solutions in the space of polynomials of degree m

$(m = 0 \rightarrow \lambda = 2, \ \psi^{(0)} = 1)$. For all other β $(\neq -m/2, \neq 1)$ the eigenfunction of (5.3) possesses a branch cut along the negative real axis $(\beta = +\tfrac{1}{2}$ is of this sort, and, so far as we know, no analytic solution has been obtained).

Let us proceed to determine the nature of the phase transition. Notice by substituting $1/x$ for x in (5.3), since $\lambda > 0$, that

$$\psi^{(\beta)}(1/x) = x^{2\beta}\psi^{(\beta)}(x) \ . \tag{5.5}$$

Setting $x = 1$ in (5.3) we see that

$$\lambda\psi^{(\beta)}(1) = 2^{-2\beta+1}\psi^{(\beta)}(\tfrac{1}{2}) \ . \tag{5.6}$$

Should $\psi^{(\beta)}(1)$ diverge, then so too must $\psi^{(\beta)}(\tfrac{1}{2})$. Setting $x = \tfrac{1}{2}$, so too must either (or both) of $\psi^{(\beta)}(\tfrac{1}{3}), \psi^{(\beta)}(\tfrac{2}{3})$. Inductively, for $\psi^{(\beta)}$ to be finite on the rationals in $(0,1)$, it follows that $\psi^{(\beta)}(1)$ is finite. Taking now the limit as $x \rightarrow 0^+$, we have

$$(\lambda - 1)\psi^{(\beta)}(0^+) = \psi^{(\beta)}(1) \ , \tag{5.7}$$

so that for $\beta < 1$ (and hence $\lambda > 1$), $\psi(0^+)$ is also finite, so that by (5.5)

$$\psi^{(\beta)}(x) \underset{x \rightarrow +\infty}{\sim} \frac{\psi^{(\beta)}(0^+)}{x^{2\beta}} \ , \tag{5.8}$$

and $\psi^{(\beta)}$ possesses an extension to $(1, \infty)$. For $\beta = 1 - \epsilon/2$, $\psi^{(\beta)}$ departs from $1/x^2$ at large x by an abrupt change of asymptotic behavior, and at $x = 0$ by becoming finite of order $1/(\lambda - 1)$. In particular, it remains smooth at $x = 1$, and we adopt the normalization

$$\psi^{(\beta)}(1) \equiv 1 \ . \tag{5.9}$$

[Indeed, by differentiating (5.5), we learn that $\psi'^{(\beta)}(1) = -\beta$].

Employ the symmetry (5.5) to rewrite (5.3) as

$$\lambda(\beta)\psi^{(\beta)}(x) = \psi^{(\beta)}(1+x) + \frac{1}{x^{2\beta}}\psi^{(\beta)}\left[1 + \frac{1}{x}\right] \ . \tag{5.10}$$

Denoting

$$1/\lambda \equiv z \ , \tag{5.11}$$

setting $x = x + n$ in (5.10) and multiplying by z^{n+1}, we have

$$z^n\psi^{(\beta)}(x+n) - z^{n+1}\psi^{(\beta)}(x+n+1)$$
$$= \frac{z^{n+1}}{(x+n)^{2\beta}}\psi^{(\beta)}\left[\frac{x+n+1}{x+n}\right]$$
$$= \frac{z^{n+1}}{(x+n+1)^{2\beta}}\psi^{(\beta)}\left[\frac{x+n}{x+n+1}\right] \ , \tag{5.12}$$

where we again used (5.5) in the last transformation. If we now sum (5.12) over $n = 0, \ldots, \infty$, by (5.8) we have (after setting $n \rightarrow n - 1$)

$$\psi^{(\beta)}(x) = \sum_{1}^{\infty} \frac{z^n}{(x+n)^{2\beta}}\psi^{(\beta)}\left[1 - \frac{1}{x+n}\right] \ . \tag{5.13}$$

Since $\psi^{(\beta)}$ is differentiable at $x = 1$, we can rewrite (5.13) as

$$\psi^{(\beta)}(x) = \sum_{}^{\infty} \frac{z^n}{(x+n)^{2\beta}} + \sum_{}^{\infty} \frac{z^n}{(x+n)^{2\beta+1}} O(1) + \cdots$$

(5.14)

where the ellipsis represents less singular terms, with $O(1)$ linear in $\epsilon = 2(1-\beta)$.

The important observation about (5.13) is that with $\psi(1-1/(x+n)) \sim \psi(1)$ for large n the radius of convergence of the series is $z = 1$. Thus, for all $\beta > 1$ $z = 1 \to \lambda = 1 \to G(\beta) = 0$, so that after reaching $\lambda = 1$ at $\beta = 1$, G remains pinned at $G(1) = 0$, and $G'(\beta) = 0$ for $\beta > 1$ (see Fig. 7). It follows that there is a phase transition (breakdown in analyticity of G in β) at $\beta = 1$. Most importantly, the transition occurs at the radius of convergence virtually guaranteeing an infinite order transition. This phenomenon can be tracked back exactly to the "intermittency" of F_0 at $x = 0 (F_0'(0) = 1)$. Since $z = e^{G(\beta)}$, $dz/d\beta$ yields $G'(\beta)$. If we attempt to differentiate (5.14) on β at $\beta = 1$, the first term $(nz^{n-1}dz/d\beta)$ becomes logarithmically divergent, while the second (the remainder) is finite (differentiable). Thus, the singular part of (5.14) at the transition is the explicit first term. Setting $x = 1$ in (5.14) and substituting

$$z = e^{-\eta},$$

(5.15)

it is straightforward to verify that the singularity in η in the first term is $\eta \ln \eta$, so that with $\eta = -G$, and for some constant k,

$$G \ln(-G) \sim k(1-\beta).$$

(5.16)

It is worth noting that (5.16) appears numerically as a first-order transition since

$$G'(\beta) \sim \frac{k}{|\ln(1-\beta)|}$$

(5.17)

so that smooth extrapolation from $\beta < 1 - \epsilon$ yields a finite $G'(1^-)$ from the slowness of variation of the logarithm and its nonanalyticity. With the presence of logarithms, unless the asymptotic form is known, all extrapolation is risky and misleading.
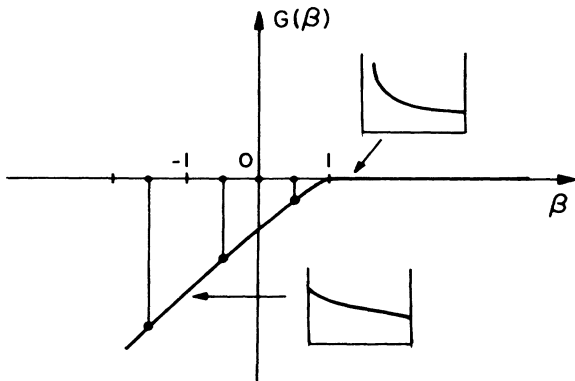

FIG. 7. A sketch of the thermodynamics of the intermittent map (5.1). At the half integers (indicated points) we possess analytic solutions.

Finally, it is worth noting that a special family of intermittent maps, those characterized by a cusp [recursion (3.1) with $z = \frac{1}{2}$ is an example], might possess normalizable invariant densities.[28] This family exhibits a first order phase transition[18] at $\beta = 1$.

VI. INCOMPLETE TREES

In this chapter we examine the formalism developed above in the context of sets that cannot be organized on complete trees. For concreteness we draw our examples from the dynamics of maps of the interval that are not Smale-complete. For one-hump maps, one knows[22] that by ordering the itineraries (symbolic dynamics) of all the points in a proper way, the itinerary of the critical point is the largest allowed one. Thus there are fewer than 2^n allowed itineraries of n symbols and the binary tree on which we can organize the preimages of the critical point is severely pruned.[33]

We shall examine a number of pruned trees. The first case will treat parameter values for which the critical point falls on an unstable periodic orbit (Misiurewicz points).[34] The second case will deal with situations in which the itinerary of the critical point is periodic (superstable orbit) and the last case is the rather general situation where the itinerary of the critical point is aperiodic.

To deal effectively with all these cases, we have to return to the derivation of the eigenvalue equation, and write a slightly more general equation that would allow effective use of the rules for pruning.

Consider again Eq. (2.11). Choosing $x = F_{\epsilon_1}(\tilde{x})$ we get

$$\lambda(\beta)\psi^{(\beta)}(F_{\epsilon_1}(\tilde{x})) = \sum_{\epsilon} |F_\epsilon'(F_{\epsilon_1}(\tilde{x}))|^{(\beta)}\psi^{(\beta)}(F_\epsilon(F_{\epsilon_1}(\tilde{x}))) .$$

(6.1)

Denoting now

$$\psi^{(\beta)}(F_\epsilon(x)) \equiv \psi_\epsilon^{(\beta)}(x) ,$$

(6.2)

Eq. (6.1) takes on the form

$$\lambda(\beta)\psi_{\epsilon_1}^{(\beta)}(x) = \sum_{\epsilon} |F_\epsilon'(F_{\epsilon_1}(x))|^{\beta}\psi_\epsilon^{(\beta)}(F_{\epsilon_1}(x)) .$$

(6.3)

The rules for pruning will be given as allowed sequences $\epsilon\epsilon_1$ in this equation. It will be seen that all the examples treated here can be brought to such a form, allowing ϵ to take on a sufficient number of values $0, 1, \ldots, k-1$.

A. Misiurewicz points

The simplest situation of this type is when the critical point is mapped (in two steps) onto the fixed point of the iteration. For maps of the type $x' = 1 - ax^2$ this occurs at $a = 1.543\,688\ldots$ The situation is depicted in Fig. 8. For convenience, we denote symbolically the interval $[1-a, 0]$ by $\epsilon = 0$, and the intervals $(0, x_0]$ and $(x_0, 1]$ by $\epsilon = 1$ and $\epsilon = 2$, respectively. Denoting the inverses of the maps, restricted to these intervals by F_0, F_1, and F_2, respectively, it is easy to check that points in 0 and 1 have inverses only in 2, whereas, points in 2 have inverses only in 0 and
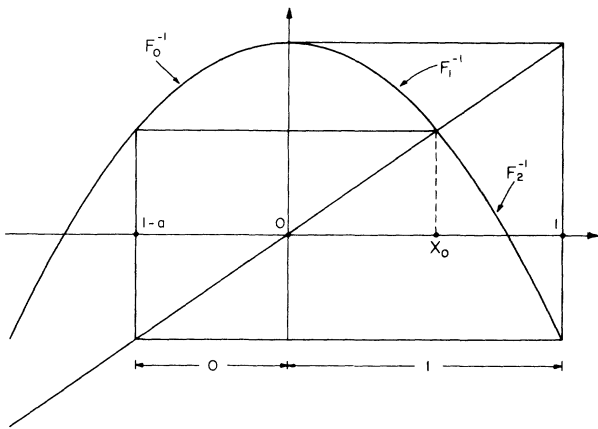
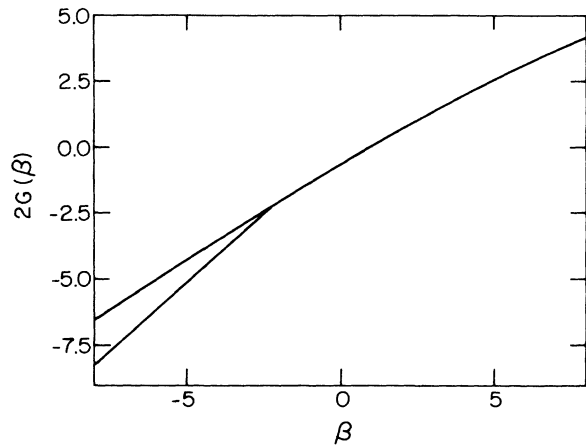FIG. 8. The situation at the first Misiurewicz point.

FIG. 9. Thermodynamics at the first Misiurewicz point. The smooth line avoids the phase transitions by taking a singular initial condition. The straight line segment belongs to the condensed phase.

1. Accordingly, Eq. (6.3) translates immediately to the set of coupled equations

$$\lambda(\beta)\psi_0^{(\beta)}(x) = |F_2'(F_0(x))|^\beta \psi_2^{(\beta)}(F_0(x)) \ ,$$

$$\lambda(\beta)\psi_1^{(\beta)}(x) = |F_2'(F_1(x))|^\beta \psi_2^{(\beta)}(F_1(x)) \ , \qquad (6.4)$$

$$\lambda(\beta)\psi_2^{(\beta)}(x) = |F_0'(F_2(x))|^\beta \psi_0^{(\beta)}(F_2(x))$$

$$+ |F_1'(F_2(x))|^\beta \psi_1^{(\beta)}(F_2(x)) \ .$$

Noticing that $F_1(x) = F_2(x) = -F_0(x)$, we can, denoting $F_1(x) = F(x)$, rewrite Eqs. (6.4) as

$$\lambda^2(\beta)\psi^{(\beta)}(x)$$

$$= |F'(x)|^\beta [|F'(F(x))|^\beta \psi^{(\beta)}(F(F(x)))$$

$$+ |F'(-F(x))|^\beta \psi^{(\beta)}(F(-F(x)))] \ , \quad (6.5)$$

where $\psi^{(\beta)}(x) = \psi_2^{(\beta)}(f(x))$. Equation (6.5) can be solved using similar techniques (like recursive functions calls) as those used previously.

To speed up the convergence one can start with an initial function that is singular at $x = 1 - a$ and $x = 1$, e.g.,

$$\tilde\psi(x) = \{[x - (1-a)](1-x)\}^{-\beta/2} \ . \qquad (6.6)$$

Such singularities should build up anyway by the iteration, and starting with them in $\tilde\psi(x)$ speeds up the convergence.

From the point of view of scaling behavior, we expect a phase transition at β negative, due to the dilation of lengths at the critical point. Any point being δ close to $x = 1$ comes from a distance $\delta^{1/2}$ near the critical point. This strong dilation results in making the neighborhood of x_0 atypical, and for β sufficiently negative this atypical behavior dominates.

We can remove the phase transition by starting with an initial function that is singular also at x_0, i.e., $\{[x - (1-a)](1-x)|x - x_0|\}^{-\beta/2}$. with such a function and β negative, we remove all the influence of the dilation at x_0. There is no path for $\beta < 0$ that leads back to the fixed point. Indeed, having such an initial function, we compute the smooth function depicted in Fig. 9. The

other line in Fig. 9 is obtained from the initial function (6.6). The phase transition is obvious. Other Misiurewicz points can be treated under similar footing and will not be detailed here.

B. Superstable orbits

When the itinerary of the critical point is periodic we have a superstable orbit. The set of interest is then not an attractor but a repeller.[35–38,23] An example is the map $1 - ax^2$ at $a_3 = 1.75488 \ldots$, which supports a superstable 3-orbit. We denote the region $[(1-a),0]$ by 0 and the region $(0,1]$ by 1. Observation shows (see Fig. 10) that 0 has preimages in 1 only, whereas 1 has preimages both in 0 and 1. We can thus write immediately

$$\lambda(\beta)\psi_0^{(\beta)}(x) = |F_1'(F_0(x))|^\beta \psi_1^{(\beta)}(F_0(x)) \ , \qquad (6.7)$$

$$\lambda(\beta)\psi_1^{(\beta)}(x) = |F_0'(F_1(x))|^\beta \psi_0^{(\beta)}(F_1(x))$$

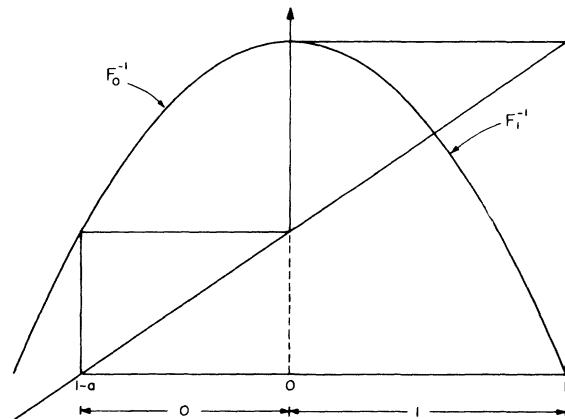$$+ |F_1'(F_1(x))|^\beta \psi_1^{(\beta)}(F_1(x)) \ , \qquad (6.8)$$

FIG. 10. The situation at a parameter value where period 3 is superstable.

where again

$$F_1(x) = \left[\frac{1-x}{a} \right]^{1/2} = -F_0(x) \; .$$

These equations can be solved using similar techniques to all previous equations.

It is interesting to notice that the numerical solution for λ_n of (3.7) converges in an oscillatory fashion, with a period 3. The reason is obvious, and stems from the fact that arbitrary initial conditions are "imbalanced" with respect to the invariant measure. A simply convergent series can be obtained by considering the averages

$$\overline{\lambda}_n = (\lambda_n \lambda_{n-1} \lambda_{n-2})^{1/3} \; . \tag{6.9}$$

These quantities converge well and approach $\lambda(\beta)$.

The convergence can be sped up again by starting with a singular function. It is easy to see from Eq. (3.4) that the required singularity is now not the "natural" one $\sigma = \beta/2$, since for $y \to 1$ we have

$$\psi_{n+1}^{(\beta)}(y) \underset{y \to 1}{\approx} \frac{\psi_n^{(\beta)} \left[\left[\frac{1-y}{a} \right]^{1/2} \right]}{\left[\frac{1-y}{a} \right]^{\beta/2}} \; . \tag{6.10}$$

If we start with $\tilde{\psi}(x) \sim x^{-\sigma}$, we get upon iteration

$$\psi^{(\beta)}(y) \underset{y \to 1}{\sim} (1-y)^{-\sigma/2-\sigma} \; . \tag{6.11}$$

However, after three further steps this singularity is transferred to $x = 0$, and, therefore,

$$\psi^{(\beta)}(y) \underset{y \to 1}{\sim} (1-y)^{-(3/4)\sigma-\sigma} \sim (1-y)^{-(7/4)\sigma} \; . \tag{6.12}$$

In the limit the singularity becomes $2\sigma = \beta$. Thus the singular function that is chosen to speed up convergence is, e.g.,

$$\tilde{\psi}(x) \equiv \{ [x - (1-a)](1-x) \}^{-\beta} \times \begin{cases} x^{-\beta} & \text{for } x > 0 \\ 1 & \text{for } x < 0 \; . \end{cases} \tag{6.13}$$

The different behavior for $x \to 0$ from above and from below stems from the fact that for $y < 0$ there is only one preimage, whereas for $y > 0$ there are two. This corresponds to an initial condition $\psi_i(x) = \tilde{\psi}(F_i(x))$, $i = 1, 2$ in Eqs. (6.7) and (6.8).

Upon iterations, starting with this initial function, fast convergence is observed. We find quantitative agreement with previous calculations[38] of the escape rate from the repeller α, the Lyapunov exponent restricted to the repeller Λ and its fractal dimension D_0. These quantities are calculated from[24]

$$G(1) = \alpha \; ,$$

$$\frac{dG(\beta)}{d\beta} \bigg|_{\beta=1} = \Lambda \; , \tag{6.14}$$
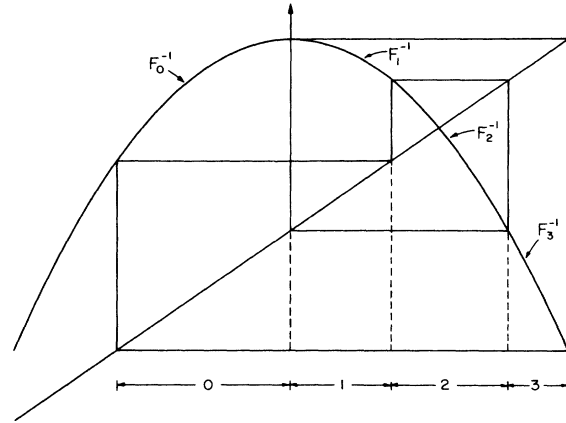
$$G(D_0) = 0 \; .$$

FIG. 11. Same as Fig. 10, for superstable period 5.

C. Aperiodic itineraries

When the itinerary of the critical point is aperiodic, it is not easy to write down a closed form theory. This problem can be circumvented by calculating the thermodynamic functions at a series of parameters for which the itinerary is periodic, a series that converges to the parameter at which the itinerary is aperiodic. As an example consider the parameter value for which the itinerary of the critical point is the same as the itinerary of a golden-mean rotation, properly reordered for one-hump maps.[39] As is well known, the golden mean is the limit of ratios of Fibonacci numbers F_n/F_{n+1}. Thus a strategy suggests itself: we can look at the thermodynamic functions at parameter values corresponding to superstable orbits of length $3, 5, 8, 13, \ldots$, and these should converge to the thermodynamic functions of the map with the above aperiodic itinerary. The period 3 case was discussed in Sec. VI B. The period 5 problem is sketched in Fig. 11. It is easy to verify that the following equations are obtained:

$$\lambda(\beta)\psi_0^{(\beta)}(x) = |F_3'(F_0(x))|^\beta \psi_3^{(\beta)}(F_0(x)) \; ,$$

$$\lambda(\beta)\psi_1^{(\beta)}(x) = |F_2'(F_1(x))|^\beta \psi_2^{(\beta)}(F_1(x)) \; ,$$

$$\lambda(\beta)\psi_2^{\beta}(x) = |F_0'(F_2(x))|^\beta \psi_0^{(\beta)}(F_2(x)) \tag{6.15}$$

$$+ |F_2'(F_2(x))|^\beta \psi_2^{(\beta)}(F_2(x)) \; ,$$

$$\lambda(\beta)\psi_3^{(\beta)}(x) = |F_0'(F_3(x))|^\beta \psi_0^{(\beta)}(F_3(x))$$

$$+ |F_1'(F_3(x))|^\beta \psi_1^{(\beta)}(F_3(x)) \; ,$$

with $F_1 = F_2 = F_3 = F$, $F_0 = -F$.

A similar analysis can be done for superstable orbits $8, 13, \ldots, F_n$, always yielding $F_n - 1$ coupled equations. The point is that $G(\beta)$ appears to converge nicely to a limit, see Fig. 12. We should stress that in the limit we obtain an infinity of coupled equations; it is our hope that such an infinite set can be represented by a single, nonlinear eigenvalue equation. Work to find such nonlinear equations is in progress, and will be reported elsewhere.
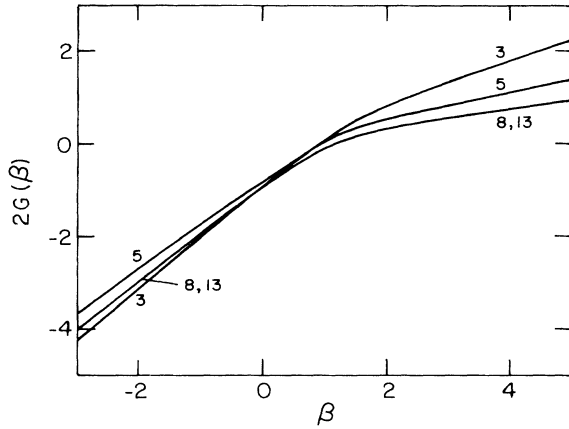
FIG. 12. Thermodynamics at superstable orbits of length 3, 5, 8, and 13. The two last ones are indistinguishable on the graph. The parameters used in $x'=1-ax^2$ are $a=1.75483$, 1.62541, 1.71108, and 1.70770, respectively.

VII. SUMMARY

The introduction of an eigenvalue equation for the calculation of the thermodynamic functions of multifractal sets has led to several results.

(i) An efficient method of computation via recursive function calls is available.

(ii) The nature of first-order phase transitions in the thermodynamic formalism has been clarified as a switch between the discrete and continuous parts of the spectra of the linear operator L.

(iii) The phase transition of the intermittent map, which is in the same class as the Farey model, the subcritical mode locking of coupled nonlinear oscillators, and a certain one-dimensional Fermi gas with logarithmic interactions, could be fully understood. The transition was shown to be of infinite order

(iv) The thermodynamics of multifractal sets which lie on incomplete trees can be efficiently computed once the pruning rules are given. The usefulness of this approach for other problems in nonlinear physics where multifractals appear will be tested in the future. Preliminary uses in the context of fractal aggregates in two dimensions indicate that the approach is efficient and worthwhile.[40]

ACKNOWLEDGMENTS

APPENDIX A: CONJUGATION

Two functions on [0,1], f and g are conjugate if

$$f(x)=h^{-1}\circ g\circ h(x) ,\tag{A1}$$

with h being a monotonous and differentiable function, with $h(0)=0$, $h(1)=1$. The invariant densities of f and g are related by

$$\psi_f^{(1)}(x)=\psi_g^{(1)}\circ h(x)|h'(x)| .\tag{A2}$$

There exists a special conjugation $\bar{h}(x)$ between $f(x)$ and $\bar{f}(x)$ such that the invariant density of $\bar{f}(x)$ is the constant function. This conjugating function $\bar{h}(x)$ is obtained as

$$\bar{h}(x)=\int_0^x \psi_f^{(1)}(x)dx .\tag{A3}$$

It has been shown that $\bar{f}(x)$ is everywhere expanding (hyperbolic) with a maximum at which the derivative of $\bar{f}(x)$ is discontinuous (tent-maplike maximum).[28]

Consider now the eigenvalue equation for two conjugate functions f and g.

$$\lambda_f \psi_f^{(\beta)}(y)= \sum_{x\in f^{-1}(y)} \frac{\psi_f^{(\beta)}(x)}{|f'(x)|^\beta} ,\tag{A4}$$

$$\lambda_g \psi_g^{(\beta)}(y)= \sum_{x\in g^{-1}(y)} \frac{\psi_g^{(\beta)}(x)}{|g'(x)|^\beta} .\tag{A5}$$

We shall show that the following statement is true:

$$\psi_f^{(\beta)}(x)=\psi_g^{(\beta)}\circ h(x)\left|\frac{dh(x)}{dx}\right|^\beta ,\tag{A6}$$

$$\lambda_f=\lambda_g .\tag{A7}$$

To see this use the identities

$$f'(x)=[h^{-1})'\circ g\circ h(x)][g'\circ h(x)h'(x)] ,\tag{A8}$$

$$(h^{-1})'\circ g\circ h(x)=\frac{1}{h'\circ h^{-1}\circ g\circ h(x)} .\tag{A9}$$

Perform now the change of variables $x=h(x')$ in Eq. (A5),

$$\lambda_g \psi_g^{(\beta)}(y)= \sum_{h(x')\in g^{-1}(y)} \frac{\psi_g^{(\beta)}(h(x'))}{|g'(h(x'))|^\beta} ,$$

$$y=g\circ h(x')=h\circ f(x') .\tag{A10}$$

Multiplying now the numerator and denominator by $|(h^{-1})'\circ g\circ h(x')h'(x')|^\beta$ and using (A9) we find

$$\lambda_g \psi_g^{(\beta)}(y)|h'\circ f(x')|^\beta$$

$$= \sum_{x'\in f^{-1}\circ h^{-1}(y)} \frac{\psi_g^{(\beta)}(h(x'))|h'(x')|^\beta}{|f'(x')|^\beta} .\tag{A11}$$

This equation is then satisfied by $\psi_f^{(\beta)}$ where

$$\psi_f^{(\beta)}(x)=\psi_g^{(\beta)}\circ h(x)\left|\frac{dh(x)}{dx}\right|^\beta\tag{A12}$$

and

$$\lambda_g=\lambda_f .\tag{A13}$$

In particular, using the special conjugation $\bar{h}$ Eq. (A3), we find

$$\psi_f^{(\beta)}(x)=\psi_f^{(\beta)}\circ \bar{h}(x)\left|\frac{d\bar{h}(x)}{dx}\right|^{\beta}$$

$$=\psi_f^{(\beta)}\circ \bar{h}(x)|\psi_f^{(1)}(x)|^{\beta} \ . \tag{A14}$$

For hyperbolic systems $\psi_f^{(\beta)}$ is smooth, and, therefore, $\psi_f^{(\beta)}(x)$ has singularities which are induced by the singularities of $\psi_f^{(1)}$ alone (see also Ref. 27). Since $\psi_f^{(1)}$ has the same singularities on both ends of strength $1-1/z$, we conclude that the eigenfunctions belonging to the discrete spectrum belong to class A.

APPENDIX B: THE FAREY MODEL AND RELATION TO INTERMITTENCY

The Farey model (also a subcritical treatment of mode-locking of coupled nonlinear oscillators;[41,16] also intermittency) is a binary tree thermodynamics with the nth set of intervals the distances between the neighbors depicted in Fig. 13. Thus, at level $n=2$ there are 2^{2-1} intervals of respective lengths $\frac{2}{5}-\frac{1}{4}$ and $\frac{3}{4}-\frac{3}{5}$. Reading from left to right at level n, the rationals encountered are in increasing order the 2^n continued fractions $[c_1,\ldots,c_k]$ of variable length k with $c_k \geq 2$ (for uniqueness of representation) satisfying

$$\sum_1^k c_i=n+2 \ , \tag{B1}$$

and each pair encountered having one element with $c_k=2$, the other with $c_k>2$. By definition,

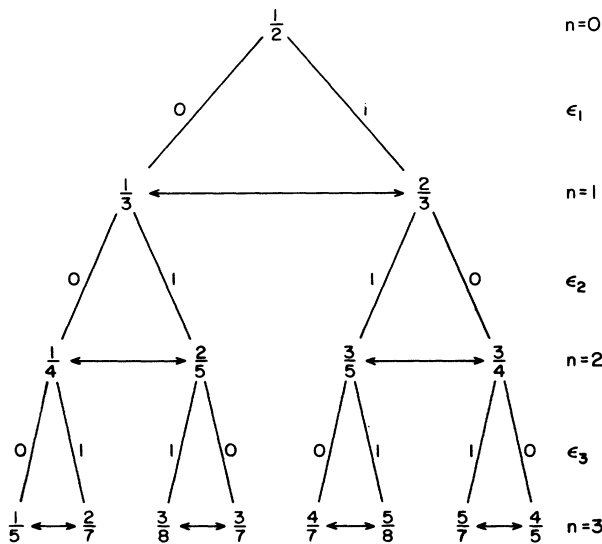$$[c_1,\ldots,c_k]=\frac{1}{c_1+[c_2,\ldots,c_k]} \ . \tag{B2}$$

FIG. 13. The Farey model. The numbers on the figure are the x values obtained via Eqs. (B7) and (B14), and the corresponding addresses $(\epsilon_n,\epsilon_{n-1},\ldots,\epsilon_1)$. Note, that an x-ordered representation of the tree is shown here and this is why the sequence of the ϵ_i's is reversed, cf. Fig. 1. The arrows indicate the balls used in the coverage [see (B10) and (2.4)] at different stages of the construction.

The tree of Fig. 13 is thus a complete enumeration of the rationals.

Let us construct the $(n+1)$th set from the nth by the following pair of rules for F_0 and F_1, respectively:

$$[c_1,\ldots,c_k]\to[c_1+1,c_2,\ldots,c_k] \ ,$$
$$[c_1,\ldots,c_k]\to[1,c_1,\ldots,c_k] \ . \tag{B3}$$

Since the sum of the c_i's is incremented by 1 by each F, by (B1) each image is in the next level; since $c_1 \geq 1$, each rational of level n produces two distinct rationals at level $n+1$. Thus, starting with [2] (level 0), any rational is obtained as

$$[c_1,\ldots,c_k]=F_0^{c_1-1}F_1F_0^{c_2-1}F_1 \cdots F_0^{c_k-1-1}F_1F_0^{c_k-2}[2] \ . \tag{B4}$$

Denoting a rational at level n by its binary index written as

$$x_i^{(n)}=x^{(n)}(\epsilon_n,\epsilon_{n-1},\ldots\epsilon_1), \quad \epsilon_j=0,1 \ , \tag{B5}$$

and ordered by the rule

$$F_\epsilon(x_i^{(n)})=x_{2i+\epsilon}^{(n+1)} \ , \tag{B6}$$

it follows that

$$x^{(n)}(\epsilon_n,\ldots\epsilon_1)=F_{\epsilon_1}\circ F_{\epsilon_2}\circ \cdots \circ F_{\epsilon_n}(x^*) \ , \tag{B7}$$

where $x^*=[2]$. Equations (B4) and (B5) now determine the binary index of $[c_1,\ldots,c_k]$ as

$$i([c_1,\ldots,c_k])$$

$$=\underbrace{0\ldots0}_{c_k-2}1\underbrace{0\ldots0}_{c_{k-1}-1}1\underbrace{0\ldots0}_{c_{k-2}-1}1\ldots1\underbrace{0\ldots0}_{c_2-1}1\underbrace{0\ldots0}_{c_1-1} \ . \tag{B8}$$

It is natural to regard the binary string of (B8) as a configuration of $k-1$ gas particles on a one-dimensional lattice of length n. It is of variable number, since $k=1,\ldots,n+1$. (For $k=n+1$ there is a unique configuration of all 1's corresponding to $[1,1,\ldots,1,2]$ with n 1's). It can be shown that a pair of rationals defining an interval, as depicted on Fig. 13, are of the form

$$[c_1,\ldots,c_k,2] \quad \text{and} \quad [c_1,\ldots,c_k+2] \ , \tag{B9}$$

and that the interval between them is of length

$$|l^{(n)}([c_1,\ldots,c_k,2])|$$

$$=\frac{[2,c_k,\ldots,c_1]^2}{\frac{2}{3}-[2,c_k,\ldots,c_1]}[c_k,\ldots,c_1]^2 \cdots [c_2,c_1]^2[c_1]^2 \ . \tag{B10}$$

The thermodynamic sum (canonical partition sum) of the model at level n is

$$\sum |l^{(n)}([c_1,\ldots,c_k,2])|^{\beta}\equiv \sum e^{-\beta H_n} \tag{B11}$$

so that

$$H_n=-\ln|l^{(n)}| \ . \tag{B12}$$

By (B10), we now have asymptotically that

$$H_n([c_1, \ldots, c_k, 2]) \sim 2 \sum_{i=1}^{k} \ln c_i + O\left[\frac{1}{c_i c_j}\right] . \quad \text{(B13)}$$

Since by (B8) the c_i's are the distances between adjacent particles, we see that the Farey model at level n is a lattice gas of varying particle number (second quantized) on a lattice of length n with long range logarithmic interaction saturating at the nearest particle. Notice that the *smallest* value of H_n is obtained with $c_1 = n \rightarrow H_n \sim 2 \ln n$, where, for all $c_i = 1$, $H_n \sim 2n \ln \rho^{-1}$ [where $\rho^{-1} = (\sqrt{5}+1)/2$] possesses the *largest* value of H_n. Thus, if the model possesses a phase transition (with $n \rightarrow \infty$, of course), its nature is that there is 0 density below a critical temperature, and finite density above it, with each site occupied (density 1) as $T \rightarrow -0$ ($\beta \rightarrow -\infty$). Thus, the model is reminiscent of a second-quantized Fermi gas (repulsive, with occupation number per site no more than one). Indeed, it is shown in Sec. V that there is a phase transition (at $\beta = 1$) of infinite order in this model.

The connection of this model to mode locking is a consequence of Farey addition (e.g., $\frac{1}{3} \oplus \frac{2}{5} = (1+2)/(3+5) = \frac{3}{8}$, look at Fig. 13) which determines that rational of smallest denominator (and hence largest mode-locking interval) lying between two given rationals numbers, and has been discussed elsewhere.[41,16] The connection to intermittency, and the solution of the model rest upon the F's of (B3), which we now work out.

Denote $[c_1, \ldots, c_k]$ by x in (B3). It follows from (B2) that

$$F_0(x) = \frac{x}{1+x} ,$$
$$F_1(x) = \frac{1}{1+x} = 1 - F_0(x) . \quad \text{(B14)}$$

Each branch is a hyperbole with

$$F_0^{-1}(x) = \frac{x}{1-x} . \quad \text{(B15)}$$

Notice that F_0 has derivative $+1$ at its fixed point $x = 0$, so that $|F_\epsilon'(x)| < 1$ is marginally violated (i.e., a multiplicative scaling converging to 1 at an end point). Indeed, (B15) is the fixed point of the "intermittency renormalization group ", so that up to our proviso on measures, we are, in this model, also working out the thermodynamics of intermittency (the precise form of the "reinjection" given by F_1^{-1} is inessential).

*Permanent address: Institute of Theoretical Physics, Eotvos University, H-1088 Budapest VIII, Hungary.

[1]M. J. Feigenbaum, Commun. Math. Phys. (1980).

[2]H. G. E. Hentschel and I. Procaccia, Physica D **8**, 435 (1983).

[3]U. Frisch and G. Parisi, in *Turbulence and Predictability in Geophysical Fluid Dynamics and Climate Dynamics*, edited by M. Ghil, R. Benzi, and G. Parisi (North-Holland, Amsterdam 1985).

[4]T. C. Halsey, M. H. Jensen, L. P. Kadanoff, I. Procaccia, and B. I. Schraiman, Phys. Rev. A **33**, 1141 (1986).

[5]G. H. Gunaratne and I. Procaccia, Phys. Rev. Lett. **59**, 1377 (1987).

[6]R. Benzi, G. Paladin, G. Parisi, and A. Vulpiani, J. Phys. A **17**, 352 (1984).

[7]T. C. Halsey, P. Meakin, and I. Procaccia, Phys. Rev. Lett. **56**, 854 (1986).

[8]C. Amitrano, A. Coniglio, and F. diLiberto, Phys. Rev. Lett. **57**, 1016 (1986).

[9]A. Coniglio, Physica A **104**, 51 (1986).

[10]J. P. Eckmann and D. Ruelle, Rev. Mod. Phys. **67**, 617 (1985).

[11]M. J. Feigenbaum, J. Stat. Phys. **46**, 919 (1987); **46**, 925 (1987).

[12]M. J. Feigenbaum, M. H. Jensen, and I. Procaccia, Phys. Rev. Lett. **56**, 1503 (1986).

[13]M. H. Jensen, L. P. Kadanoff, and I. Procaccia, Phys. Rev. A **36**, 1409 (1987).

[14]D. Ruelle, *Thermodynamic Formalism* (Addison-Wesley, Reading, 1978); R. Bowen, *Equilibrium States and the Ergodic Theory of Anosov Diffeomorphisms*, Vol. 470 of *Lecture Notes in Mathematics* (Springer, New York, 1975), p. 1; Ya. Sinai, Russ. Math. Surv. **166**, 21 (1972).

[15]T. Bohr and D. Rand, Physica D **25**, 387 (1987).

[16]P. Cvitanovic, in *Proceedings of the XV International Colloquim on Group Theoretical Methods in Physics*, edited by R. Gilmore (World Scientific, Singapore, 1987).

[17]D. Katzen and I. Procaccia, Phys. Rev. Lett. **58**, (1987).

[18]P. Szepfalusy, T. Tel, A. Csordas, and Z. Kovacs, Phys. Rev. A **36**, 3525 (1987).

[19]P. Grassberger, R. Badii, and A. Politi, J. Stat. Phys. **51**, 135 (1988).

[20]M. J. Feigenbaum (unpublished); T. Bohr and M. H. Jensen, Phys. Rev. A **36**, 4904 (1987).

[21]M. J. Feigenbaum *Complex Objects on Regular Trees*, Proceedings of the 1987 NATO Summer School (Plenum, New York, 1987).

[22]P. Collet and J. P. Eckmann, *Iterated Maps on the Interval as Dynamical Systems* (Birkhauser, Basel, 1980).

[23]P. Szepfalusy and T. Tel, Phys. Rev. A **34**, 2520 (1986); T. Tel, Phys. Lett. A **119**, 65 (1986); T. Tel, Phys. Rev. A **36**, 1502 (1987).

[24]T. Tel, Phys. Rev. A **36**, 2507 (1987).

[25]P. Grassberger and I. Procaccia, Phys. Rev. A **28**, 2591 (1983).

[26]G. Györgyi and P. Szépfalusy, J. Stat. Phys. **34**, 451 (1984).

[27]A. Csordás and P. Szépfalusy, Phys. Rev. A **38**, 2582 (1988).

[28]G. Györgyi and P. Szépfalusy, Z. Phys. B **55**, 179 (1984).

[29]P. Szépfalusy and T. Tél, Phys. Rev. A **35**, 477 (1987).

[30]T. Bohr and T. Tél, in *Directions in Chaos*, edited by U. Bai-Lin Hao (World Scientific, Singapore, 1988), Vol. II.

[31]P. Manneville and Y. Pomeau, Physica D **1**, 219 (1980).

[32]J. E. Hirsch, M. Nauenberg, and D. J. Scalapino, Phys. Lett. **87A**, 391 (1982).

[33]P. Cvitanovic, G. H. Gunaratne, and I. Procaccia, Phys. Rev. A **38**, 1503 (1988).

[34]M. Misiurewicz, Publ. Math. IHES **53**, 17 (1981).

[35]D. Ruelle, Ergod. Th. Dynam. Syst. **2**, 99 (1982).

[36]M. Widom, D. Bensimon, L. P. Kadanoff, and S. J. Shenker, J. Stat. Phys. **32**, 443 (1983).

[37]L. P. Kadanoff and C. Tang, Proc. Natl. Acad. Sci. U.S.A. **81**, 1276 (1984).

[38]H. Kantz and P. Grassberger, Physics D **17**, 75 (1985).

[39]I. Procaccia, S. Thomae, and C. Tresser, Phys. Rev. A **35**, 1884 (1987).

[40]I. Procaccia and R. Zeitak, Phys. Rev. Lett. **60**, 2511 (1988).

[41]M. H. Jensen, P. Bak, and T. Bohr, Phys. Rev. Lett. **50**, 1637 (1983); Phys. Rev. A **30**, 1960 (1984).